Journal of Electrochemistry

Volume 30 | Issue 8

2024-08-28

Recent Advances on Ruthenium-Based Electrocatalysts for Lithium-Oxygen Batteries

Yu-Zhe Wang

Zhuo-Liang Jiang

Bo Wen

Yao-Hui Huang

Fu-Jun Li
a Frontiers Science Center for New Organic Matter, Key Laboratory of Advanced Energy Materials Chemistry (Ministry of Education), College of Chemistry, Nankai University, Tianjin 300071, China; b Haihe Laboratory of Sustainable Chemical Transformations, Tianjin 300192, China, fujunli@nankai.edu.cn

Recommended Citation

Yu-Zhe Wang, Zhuo-Liang Jiang, Bo Wen, Yao-Hui Huang, Fu-Jun Li. Recent Advances on Ruthenium-Based Electrocatalysts for Lithium-Oxygen Batteries[J]. *Journal of Electrochemistry*, 2024 , 30(8): 2314004.
DOI: 10.61558/2993-074X.3466
Available at: https://jelectrochem.xmu.edu.cn/journal/vol30/iss8/1

REVIEW

Invited Contribution from Award Winners of the 21st National Electrochemical Congress in 2023

Recent Advances on Ruthenium-based Electrocatalysts for Lithium-oxygen Batteries

Yu-Zhe Wang [a], Zhuo-Liang Jiang [a], Bo Wen [a], Yao-Hui Huang [a], Fu-Jun Li [a,b,*]

[a] Key Laboratory of Advanced Energy Materials Chemistry (Ministry of Education), College of Chemistry, Nankai University, Tianjin 300071, China
[b] Haihe Laboratory of Sustainable Chemical Transformations, Tianjin 300192, China

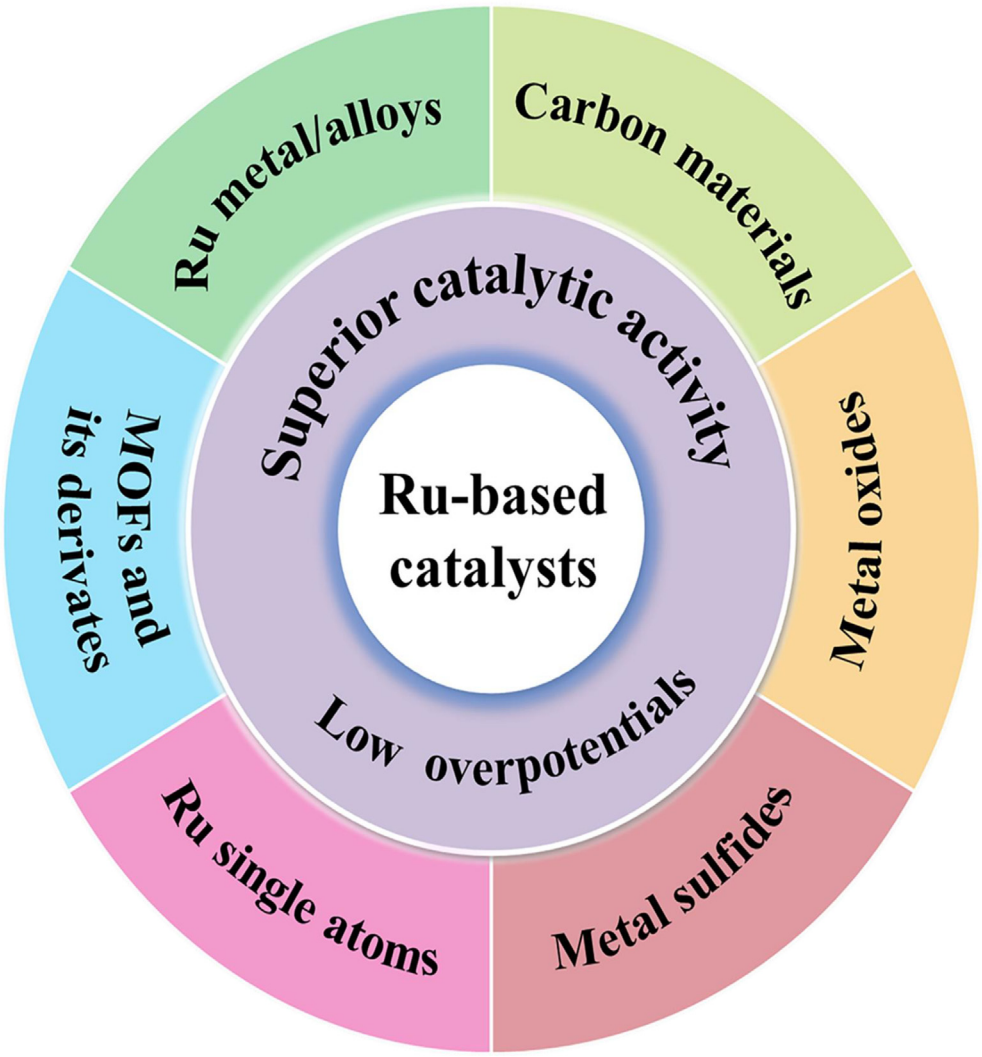

Received 24 December 2023; Received in revised form 22 April 2024; Accepted 26 April 2024
Available online 29 April 2024

* Corresponding author, Fu-Jun Li, E-mail address: fujunli@nankai.edu.cn.

https://doi.org/10.61558/2993-074X.3466

Abstract

Rechargeable lithium-oxygen (Li-O_2) batteries have attracted wide attention due to their high energy density. However, the sluggish cathode kinetics results in high overvoltage and poor cycling performance. Ruthenium (Ru)-based electrocatalysts have been demonstrated to be promising cathode catalysts to promote oxygen evolution reaction (OER). It facilitates decomposition of lithium peroxide (Li_2O_2) by adjusting Li_2O_2 morphologies, which is due to the strong interaction between Ru-based catalyst and superoxide anion (O_2^-) intermediate. In this review, the design strategies of Ru-based electrocatalysts are introduced to enhance their OER catalytic kinetics in Li-O_2 batteries. Different configurations of Ru-based catalysts, including metal particles (Ru metal and alloys), single-atom catalysts, and Ru-loaded compounds with various substrates (carbon materials, metal oxides/sulfides), have been summarized to regulate the electronic structure and the matrix architecture of the Ru-based electrocatalysts. The structure-property relationship of Ru-based catalysts is discussed for a better understanding of the Li_2O_2 decomposition mechanism at the cathode interface. Finally, the challenges of Ru-based electrocatalysts are proposed for the future development of Li-O_2 batteries.

Keywords: Lithium-oxygen battery; Ruthenium-based electrocatalyst; Reaction mechanism; Reaction kinetics; Overvoltage

1. Introduction

Rechargeable lithium-oxygen (Li-O_2) batteries have an ultrahigh theoretical energy density of 3500 $Wh \cdot kg^{-1}$, which is based on the reduction of O_2 and formation/decomposition of Li_2O_2 [1,2]. During the discharge, Li_2O_2 can be generated via solution-mediated model or surface-adsorption model. Toroid-shaped Li_2O_2 will be formed via disproportionation or a second one-electron electrochemical reduction of soluble LiO_2 intermediate in the solution-mediated model. Film-like Li_2O_2 will be formed via a surface-adsorption model due to the strong affinity between LiO_2 intermediate and cathodes. During the charge, Li_2O_2 is decomposed to produce O_2. However, the heterogeneity of three-phase interfaces hinders the mass and electronic transportation, resulting in the sluggish oxygen reduction reaction (ORR) and oxygen evolution reaction (OER) kinetics. The discharge product of Li_2O_2 is characterized by a low electronic conductivity and this leads to increased interfacial impedance. The incomplete Li_2O_2 decomposition gradually blocks the cathode surface and induces capacity decay [3,4]. Moreover, the insulated Li_2O_2 causes high charging overvoltage and low round-trip efficiency, which promotes the formation of reactive oxygen species such as singlet oxygen ($^1O_2$). The generated reactive species can easily attack the electrolytes and electrode materials, leading to by-product accumulation on the cathode surface. The catalytic activity of cathode materials is therefore suppressed due to the blocked reaction sites [5,6]. It is essential to design novel catalysts with superior OER kinetics to decrease the charging overpotential for stable Li-O_2 batteries.

Various materials have been employed as cathode catalysts to reduce discharge/charge overpotentials in Li-O_2 batteries, such as: carbon materials, noble metals and transition metal oxides [7−9]. Carbon materials have gained much attention due to their high surface area and low production cost. However, they are prone to react with electrolyte, and generate by-product like lithium carbonate (Li_2CO_3). The side reactions quickly lead to capacity degradation and a low round-trip efficiency [10−12]. Ru-based materials are considered as a more efficient catalyst owing to their strong interaction with oxygen species intermediate [13−15]. This leads to adjustment of reaction routes and enhances the OER kinetics, decreasing the charge overpotential to less than 0.5 V. The intensive adsorption between superoxide anion (O_2^-) and Ru active sites can significantly affect the Li_2O_2 growth and change its morphologies (toroid/film). Different Li_2O_2 morphologies are endowed with varied electronic transport and interfacial impedance, which finally leads to different charge overvoltages. The adsorption energy and charge transfer barrier are closely related to mass diffusion and electrophilicity of the catalytic sites [16−20]. Therefore, matrix architecture is usually designed to increase the catalyst surface area for enhancing electron and reactant diffusions [21], while electronic structure is tuned to increase the interaction between catalyst and intermediates [22−24]. Unfortunately, the excessive catalytic effect of Ru-based materials may decompose organic electrolyte and the high production cost of noble metal limits its practical application. It is essential to construct suitable structures to regulate Ru catalytic property and increase the utilization efficiency of Ru sites.

Although the Ru-based catalysts exhibit great potential to enhance the OER kinetics, the Li-O_2 battery still has poor cycling stability and Ru catalytic efficiency should be further improved.

Understanding reaction mechanism of Li_2O_2 decomposition on the cathode is necessary to fully taking advantage of Ru-based catalysts for reducing the charging overpotential. This review has summarized various configurations of Ru-based catalysts, including metal particles, single atom catalyst, and Ru-based compounds with different substrates, in boosting OER kinetics of Li-O_2 battery. Regulation of intermediate adsorption and catalyst electronic structure is introduced to control the Li_2O_2 morphology and decrease the interfacial impedance. Some perspectives are presented for the further development of reliable Ru-based catalysts to realize long-term stable Li-O_2 battery.

2. Design and modulation of Ru-based electrocatalysts

2.1. Ru metal and alloys

Precious metals and their alloys exhibit excellent ORR and OER performances, and therefore, they have been widely utilized as cathode catalysts in the preliminary research of Li-O_2 batteries [13–15]. Su et al. designed hierarchical Ru nanospheres as cathode catalysts for Li-O_2 batteries by a simple hydrothermal method [25]. The hierarchical Ru nanospheres with large surface area increased catalytic active sites, promoting the reversible generation and decomposition of the leaf-like Li_2O_2. The Li-O_2 batteries based on the hierarchical Ru nanospheres cathode displayed a low overpotential (0.3 V) at 200 $mA \cdot g^{-1}$. However, precious metal damages the reversibility of the battery. Peng and his collaborators loaded Ru metal onto carbon nanotubes as the cathode catalyst for Li-O_2 battery [26]. As illustrated in the transmission electron microscopic (TEM) image in Fig. 1a, carbon nanotubes are found to be fully covered by Ru nanoparticles. This endowed the Li-O_2 battery with a low charge overpotential of 0.53 V and a long lifespan of 100 cycles (Fig. 1b). They then further investigated the reversibility of Li-O_2 batteries with differential electrochemical mass spectrometry (DEMS). They reported that the charge to O_2 ratio (e^-/O_2) equaled 2.08 during the discharge, which is very close to theoretical $2e^-/O_2$ (Fig. 1c). However, the e^-/O_2 value increased to 3.14 during the charge, with a massive amount of CO_2 generated (Fig. 1d). This phenomenon suggests that strong catalytic activity and poor selectivity of Ru catalyst can result in the decomposition of electrolyte during charge, posing a threat to the stability of Li-O_2 battery. An available strategy is to design suitable Ru-based compounds catalysts to boost ORR/OER performance for Li-O_2 batteries.

2.2. Carbon materials

Carbon materials with high conductivity, low cost and light weight have been extensively used as

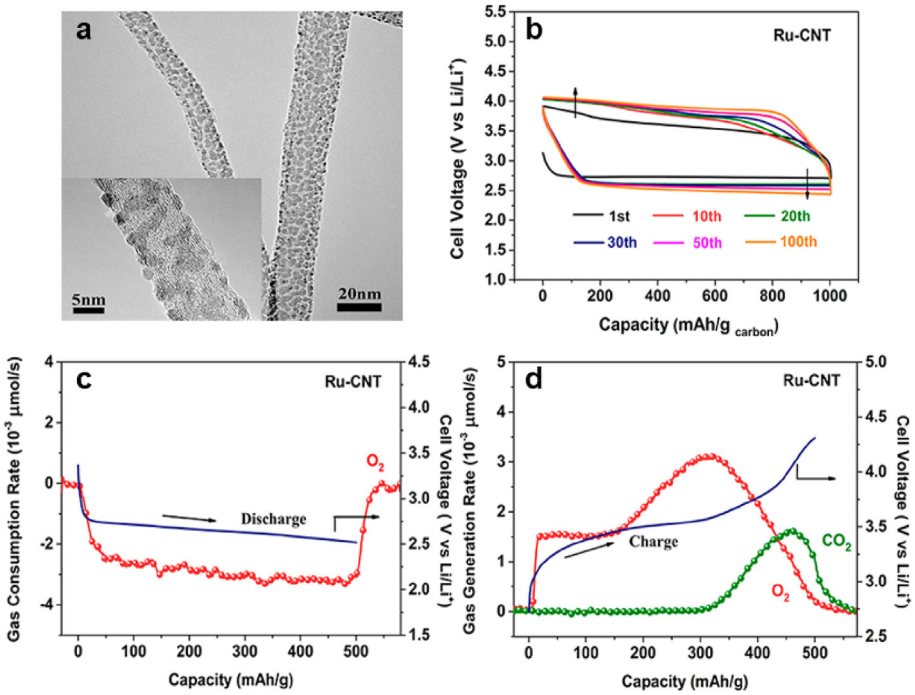

Fig. 1. (a) TEM images of Ru-CNT. (b) Multiple cycles from 1 to 100 of the catalyzed Li-O_2 cells based on Ru-CNT. (c) DEMS results of O_2 gas consumption during the discharge of Li-O_2 batteries based on Ru-CNT. (d) DEMS results of O_2 and CO_2 evolution during the charging process of Li-O_2 batteries based on Ru-CNT. Reprinted with permission of Ref. [26], copyright 2015 American Chemical Society.

cathode catalysts for Li-O_2 batteries [27–29]. However, the limited catalytic activity of carbon materials constrains the capacity of Li-O_2 batteries. Ru-based compounds with superior catalytic activity are often combined with carbon materials to form hybrid catalysts. In this hybrid system, Ru-based compounds serve as the active sites, carbon-containing materials act as the conductive medium. The synergistic effect of the two components ultimately reduces overpotential and improves cycle stability. Sun et al. synthesized carbon black-supported Ru nanocrystalline (Ru-CB) to improve the performance of Li-O_2 batteries. The Li-O_2 batteries based on Ru-CB cathode boosted the ORR and OER kinetics, and reduced the discharge/charge overpotential (0.37 V) [30].

The irregular accumulation of Li_2O_2 on the cathode covers the active sites of Ru, thereby restricting its catalytic performance. Porous carbon materials with a large surface area offer ample space for the growth of Li_2O_2. This makes Ru active sites fully utilized to promote the decomposition of Li_2O_2, enhancing the reversibility of Li-O_2 batteries. The mesoporous carbon nanocubes after loading Ru nanocrystals were designed as cathode catalysts for Li-O_2 batteries, yielding higher discharge capacity than commercial carbon black catalysts [31]. Song et al. prepared a "breathable" wood-based cathode by anchoring Ru nanoparticles on the open porous microchannels of carbonized and activated wood (CA-wood) [32]. Numerous aligned microchannels in the three-dimensional (3D) wood-based material facilitate the fast lithium ions transport, oxygen diffusion and full electrolyte infiltration. Besides, the uniformly dispersed Ru particles form numerous reactive sites to promote the formation and decomposition of Li_2O_2 (Fig. 2a). During discharging, Li_2O_2 is generated on the wall of the microchannels and covers the surface of Ru nanoparticles, as revealed in Fig. 2b and c. After charging, the formed Li_2O_2 is completely decomposed (Fig. 2d and e), showing good reversibility in the discharge/charge process. Therefore, Li-O_2 batteries based on "breathable" CA-wood/Ru-based cathode exhibited a high specific area capacity of 8.58 $mA \cdot h \cdot cm^{-2}$ at a current density of 0.1 $mA \cdot cm^{-2}$.

Previous literatures have reported that the majority of hybrid catalysts exhibit high Ru mass loading of 20 wt%–40 wt%, leading to the aggregation of Ru clusters and incomplete catalytic activity. For example, Sun et al. prepared a reduced graphene cathode with 20.34 wt% Ru nanoparticles. Wang et al. applied Ru-functionalized (43 wt%) vertical graphene nanosheets supported on a Ni-foam cathode (VGNS@NiFM) as cathode catalysts for Li-O_2 batteries. Besides, the FeCo-doped NrGO mounted with Ru nanoparticles (20 wt% loading) was synthesized as cathode catalysts for Li-O_2

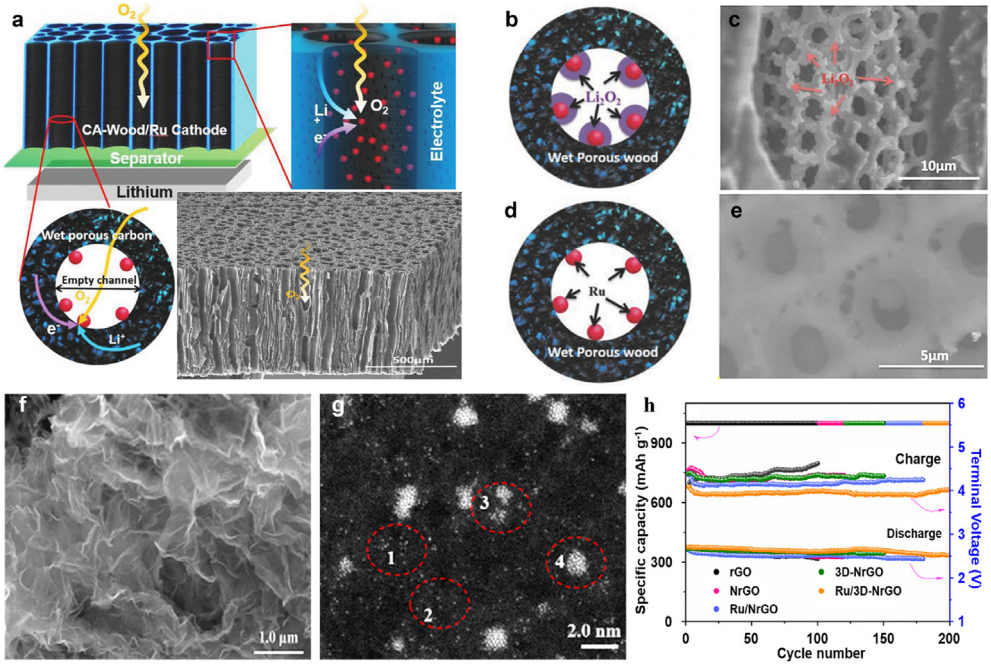

Fig. 2. (a) Schematic diagram of the Li-O_2 batteries with the CA-wood/Ru cathode. (b) Schematic diagrams showing Li_2O_2 growth during discharging. (c) SEM image showing the microchannels after the first discharge. (d) Schematic diagrams showing Li_2O_2 vanishing during charging. (e) SEM image showing the microchannels after the first charge. Reprinted with permission of Ref. [32], copyright 2018 Wiley-VCH. (f) SEM image of Ru/3D-NrGO. (g) HAADF-STEM image of Ru nanoclusters anchored on 3D-NrGO. (h) The cycling performance depending on cycle number of cathodes at a cut-off capacity of 1000 $mAh \cdot g^{-1}$ and a charge–discharge rate of 200 $mA \cdot g^{-1}$. Reprinted with permission of Ref. [33], copyright 2020 American Chemical Society.

batteries. Liu et al. fixed highly dispersed Ru nanoclusters on the 3D nitrogen-doped graphene (3D-NrGO), achieving a reduced Ru loading of 9.37 wt% (Fig. 2f and g) [33]. The 3D architecture of graphene and highly dispersed Ru greatly improved the performance of Li-O_2 batteries, resulting in large discharge capacity of 23,992 mAh·g^{-1} at 100 mA·g^{-1} and long lifespan of 200 cycles (Fig. 2h).

In addition to the physical effects of carbon materials, carbon materials can interact with Ru to modulate the local electronic structure of Ru, inducing the adsorption of LiO_2 intermediates. The suitable adsorption between Ru and LiO_2 intermediates ensures a feasible Li_2O_2 formation and decomposition route. Dai et al. adopted nitrogen-doped reduced GO anchored the well-dispersed Ru nanoparticles (Ru/N-rGO) as an efficient bifunctional catalyst for Li-O_2 batteries [34]. The N dopants within rGO boost stronger electron transfer from Ru to carbon materials (Fig. 3a). The electron-deficient Ru increases LiO_2 adsorption, leading to the generation of Li_2O_2 film during the initial discharge, and followed by the generation of Li_2O_2 particles after the subsequent deep discharge. The change of Li_2O_2 morphology is ascribed to alter the reaction interface. During charging, Li_2O_2 is easily decomposed due to its good electrical contact with Ru/N-rGO. As a result, the Li-O_2 batteries showed the reversible formation and decomposition of Li_2O_2 (Fig. 3b). However, Ru anchored on the carbon materials surface as conventional support-metal interaction is very easy to cause limit contact area, restricting the catalytic effect of Ru. A novel chimeric structure material was proposed by Sun et al. [35]. The Ru nanoparticles partially confined in the microtubular walls of carbon fabrics (Ru-chimera-CMT) expose partial surface, increasing the electron density of Ru nanoparticles and inducing the LiO_2 gradient adsorption (Fig. 3c and d). The DFT calculation describes the adsorption energy of LiO_2 on the cathode, as shown in Fig. 3e–h. The adsorption energy (ΔE_{ads}) of LiO_2 is −0.82 eV when Ru nanoparticles are anchored on graphene (Fig. 3e). On the contrary, the ΔE_{ads} of LiO_2 is −2.41 eV at Ru/graphene interface when Ru nanoparticles are partially embedded into the graphene. Different from the Ru/graphene interface, the ΔE_{ads} of LiO_2 is only −0.33 eV on the Ru center of the material (Fig. 3f). The gradient adsorption from Ru/graphene interface to Ru center induces the formations of Li_2O_2 nanosheets and particles. Such Li_2O_2 morphology fully utilizes the Ru active site upon charging, expediting Li_2O_2 decomposition (Fig. 3g and h). As a result, the Ru-chimera-CMT cathode can exhibit excellent cycling performance for Li-O_2 batteries.

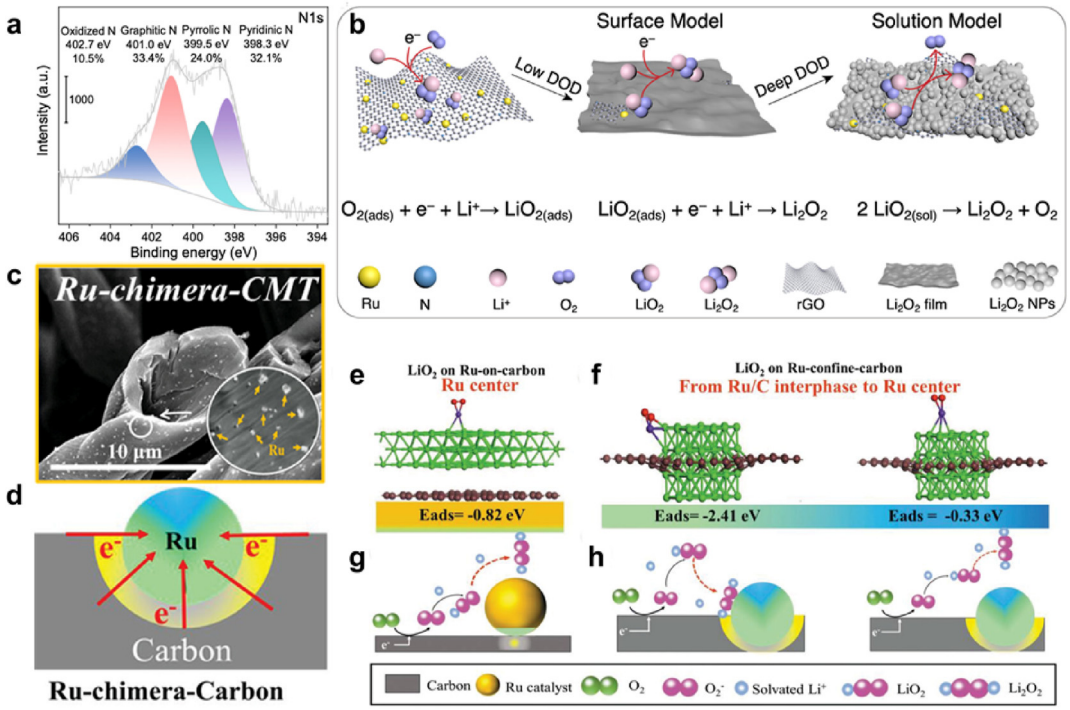

Fig. 3. (a) Deconvoluted X-ray photoelectron spectrum for the N 1s of Ru/N-rGO. (b) Schematic of the discharge mechanism for Ru/N-rGO. Reprinted with permission of Ref. [34], copyright 2021 American Chemical Society. (c) The SEM image of Ru-chimera-CMT. (d) Schematic of contact electrifications for Ru-chimera-CMT. DFT calculations and proposed mechanisms. The optimized structures of (e) LiO_2 adsorbed on (101) plane of Ru configuration in Ru-on-graphene model and (f) LiO_2 adsorbed on the Ru configuration of Ru-chimera-graphene. Discharge mechanisms of (g) Ru-on-CMT and (h) Ru-chimera CMT. Reprinted with permission of Ref. [35], copyright 2021 Wiley-VCH.

2.3. Metal oxides

Although hybrid catalysts composed of Ru-based compounds and carbon materials improve the ORR/OER kinetics and reversibility of the Li-O_2 batteries, the parasitic reactions between the electrolyte and the carbon material still need to be carefully considered [36]. The occurrence of side reactions in Li-O_2 batteries is primarily attributed to the higher charging voltage. Metal or metal oxides combined with Ru-based compounds as a carbon-free cathode can reduce the charge voltage, inhibiting the side reactions caused by high voltage. A conductive indium tin oxide (ITO) electrode embedded with Ru nanoparticles (Ru/ITO) was first introduced as a carbon-free cathode in Li-O_2 batteries by Zhou's group [37]. The Ru/ITO electrodes effectively decrease the generation of by-product, improving the cycling stability of Li-O_2 batteries. However, the Ru/ITO electrodes have the relatively low specific capacity owing to the large weight of ITO. Li et al. further prepared antimony (Sb)-doped tin oxide (STO) supported Ru nanoparticles (Ru/STO) as a carbon-free cathode for Li-O_2 batteries [38]. Compared with ITO, the Ru/STO cathode exhibited a large specific capacity of 750 mAh·g^{-1} with low overpotentials.

Various metal oxides with excellent ORR activity, including manganese (Mn)-based oxides [39], cerium dioxide (CeO_2) [40], spinel [41,42] and perovskite oxides [43], can induce the formation of discharge products with different morphologies, and Ru-based compounds are more conducive to the decomposition of discharge products with different morphologies. Therefore, metal oxides with ORR activity can combine with Ru-based compounds as bifunctional catalysts to further enhance the ORR/OER activity of Li-O_2 batteries. Manganese-based oxides have been extensively studied as excellent ORR catalysts in Li-O_2 batteries. Yoon et al. fabricated RuO_2/Mn_2O_3 fiber-in-tube (RM-FIT) and RuO_2/Mn_2O_3 tube-in-tube (RM-TIT) as bifunctional catalysts for Li-O_2 batteries, and manipulated the structures of catalysts to change the growth location of discharge products [44]. RM-FIT is composed of Mn_2O_3 as the outer tubes and most RuO_2 as the inner core. During discharge, Li_2O_2 is mainly generated on the surface of the outer tubes due to the high ORR activity of Mn_2O_3. During charge, the relatively low OER catalytic activity of Mn_2O_3 lead to the incomplete decomposition of Li_2O_2, which causes the reductions of round-trip efficiency and performance (Fig. 4a and b). On the contrary, RuO_2/Mn_2O_3

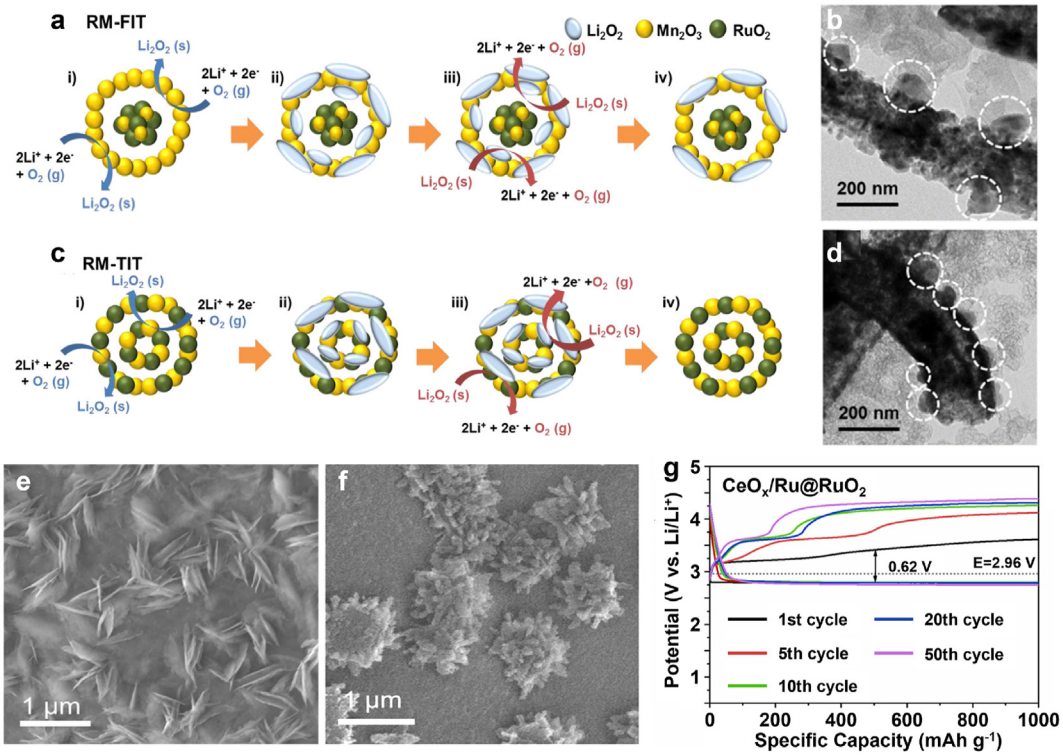

Fig. 4. (a) Proposed reaction mechanism of RM-FIT. (b) Discharged states in RM-FIT electrode during the operation of Li-O_2 cells. (c) Proposed reaction mechanism of RM-TIT. (d) Discharged states in RM-TIT electrode during the operation of Li-O_2 cells. Reprinted with permission of Ref. [44], copyright 2016 American Chemical Society. SEM images of (e) CeO_x/Ru@RuO_2 and (f) CeO_x/C after the first discharge at a limited capacity of 1000 mAh·g^{-1}; (g) Limited capacity (1000 mAh·g^{-1}) tested at 200 mA·g^{-1}: discharge/charge profiles of CeO_x/Ru@RuO_2. Reprinted with permission of Ref. [40], copyright 2022 Elsevier.

tube-in-tube (RM-TIT) consists of distributed Mn_2O_3 and RuO_2 nanocomposites in the double-walled fibers, resulting in the deposition of Li_2O_2 in the inner and outer tubes of Mn_2O_3 components. The formation of Li_2O_2 can be decomposed by adjacent RuO_2 components, enhancing the cycling and rate performances of Li-O_2 batteries (Fig. 4c and d).

Similarly, Wu et al. synthesized the hybrid nanosheets composed of sub-5nm CeO_x and $Ru@RuO_2$ nanoparticles attached to a low percentage (1.2%) antioxidant carbon as bifunctional catalysts for Li-O_2 batteries [40]. A number of Li_2O_2 nanoflakes is formed on the CeO_x/$Ru@RuO_2$ surface during the discharge (Fig. 4e), which can be completely decomposed during the charge. The phenomenon strongly suggests that the active sites of CeO_x and $Ru@RuO_2$ play a significant role in adjusting the nucleation of Li_2O_2 to form nanoflakes. These nanoflakes are helpful to O_2 diffusion and electrolyte immersion, enhancing the reversibility of Li-O_2 batteries. In contrast, a large island-like Li_2O_2 is formed on the CeO_x/C surface after the discharge (Fig. 4f), and a few particles cannot be completely decomposed on the surface after charging due to the lack of Ru-based compounds. Therefore, Li-O_2 batteries based on CeO_x/$Ru@RuO_2$ cathode catalysts exhibited very small ORR (0.17 V) and OER (0.45 V) overpotentials, a reversible capacity of over 9700 $mAh \cdot g^{-1}$ and a good cycling performance of 79 cycles at the limited capacity test of 1000 $mAh \cdot g^{-1}$ (Fig. 4g).

In order to improve the catalytic activity and durability of Ru-based compounds catalysts, the electronic metal-support interaction (EMSI) criterion has been used to rational design Ru-based compounds catalysts for Li-O_2 batteries. Lian et al. synthesized the hierarchical porous carbon shells loaded atomically distributed Fe modified RuO_2 nanoparticles (Fe_{SA}-RuO_2/HPCS) [45], as shown in Fig. 5a and b. The result by X-ray absorption spectroscopy (XAS) reveals that the Ru-O-Fe_1 structure is formed in the Fe_{SA}-RuO_2/HPCS by the electron interaction between Fe atoms and Ru sites (Fig. 5c). During the discharge, the Ru-O-Fe_1 structure leads to the negative shift of the d-band center of the Fe_{SA}-RuO_2, weakening the adsorptions of O_2 and LiO_2 on the Fe_{SA}-RuO_2 (Fig. 5d–f).

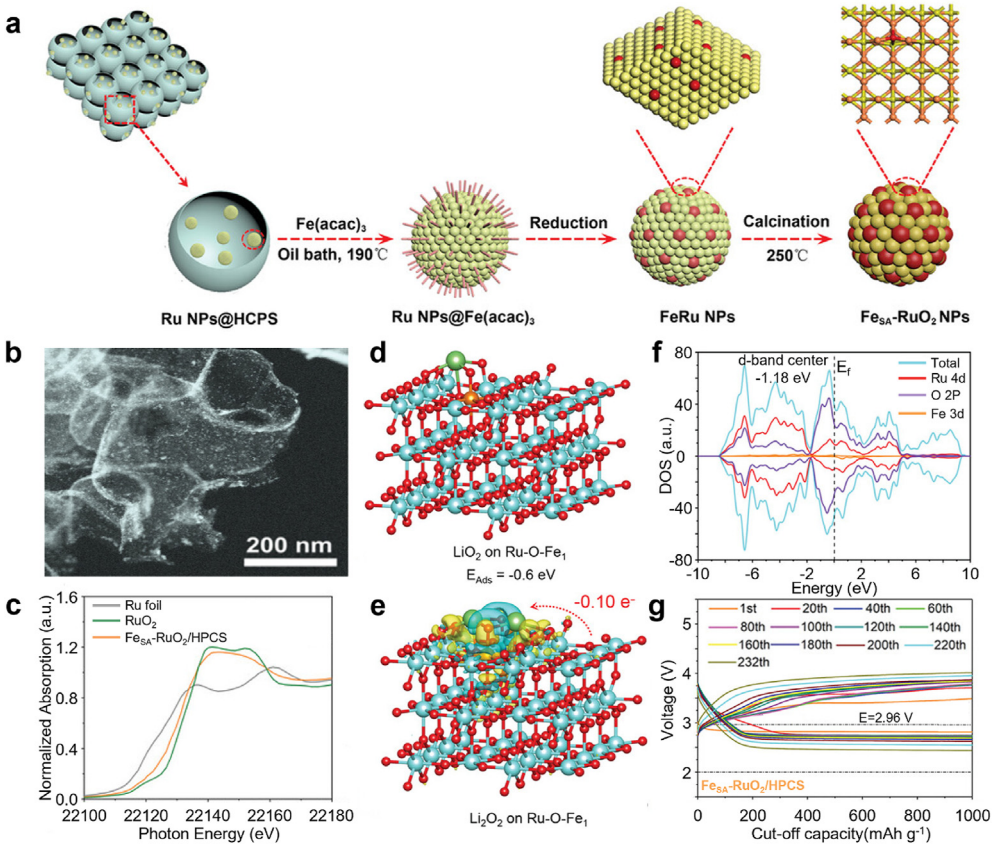

Fig. 5. (a) Schematic illustration of the synthesis process of the Fe_{SA}-RuO_2/HPCS. (b) HAADF-STEM image of Fe_{SA}-RuO_2/HPCS. (c) Ru K-edge normalized XANES spectra. (d) Adsorption energy of reaction intermediate LiO_2 on Ru-O-Fe_1 active sites. (e) Charge density differences for Li_2O_2 adsorption states and corresponding charge transfer on the Ru-O-Fe_1 active sites. (f) The total density of states (DOS) and partial density of states (PDOS) of Ru-O-Fe_1 models. (g) Discharge-charge profiles of Fe_{SA}-RuO_2/HPCS cathodes with different cycles at 200 $mA \cdot g^{-1}$ and 1000 $mAh \cdot g^{-1}$. Reprinted with permission of Ref. [45], copyright 2023 Wiley-VCH.

The suitable adsorption between Ru-O-Fe_1 structure and LiO_2 optimizes the growth Li_2O_2, improving the ORR kinetics. During the charge, Li_2O_2 is effectively decomposed by electron transfer between the Ru-O-Fe_1 sites and Li_2O_2, boosting the OER kinetics. As a result, the Li-O_2 batteries based on the Fe_{SA}-RuO_2/HPCS catalysts illustrated very low overpotential (0.34 V) and excellent cycling performance (232 cycles) (Fig. 5g).

2.4. Metal sulfides

Metal sulfides exhibit better electric conductivity, thermal and mechanical stability compared to metal oxides [46]. The ternary chalcogenides (AB_2S_4) possess the unique surface electronic properties because the metal cations of A^{2+}/B^{3+} take up the octahedral/tetrahedral sites of the tightly packed S anionic lattice [47]. The interaction between transition metal atoms and heteroatoms results in the generation of unsaturated coordination centers (M_1-M_2) by introducing S vacancy in AB_2S_4 and allowing heteroatoms to occupy S vacancy. M_1-M_2 acts as the active site to accelerate charge transfer, leading to the formation and decomposition of Li_2O_2 in Li-O_2 batteries [48].

Zheng et al. embedded Ru into the S vacancies of $CoInS_4$ to create unsaturated coordination Ru-Co active center, which is helpful to improve the reversibility of Li-O_2 batteries [49]. The synthesis method of the Ru-Vs-$CoInS_4$ (Ru-V-CIS) electrode is presented in Fig. 6a. Firstly, CIS is grown on the Carbon Cloth (CC) after hydrothermal treatment. Next, the S vacancy of CIS electrode (V-CIS) is created by $NaBH_4$, which can serve as the reduction agent to provide electrons and H^-. Finally, the Ru-Vs-$CoInS_4$ with nanosheets array is constructed by depositing Ru on the V-CIS (Fig. 6b). The false-color HRTEM image of V-CIS shows that some atoms are absent, illustrating the presence of S vacancies (Fig. 6c). Moreover, the EPR spectra detect unpaired electrons due to the formation of vacancy, verifying the production of the S vacancy

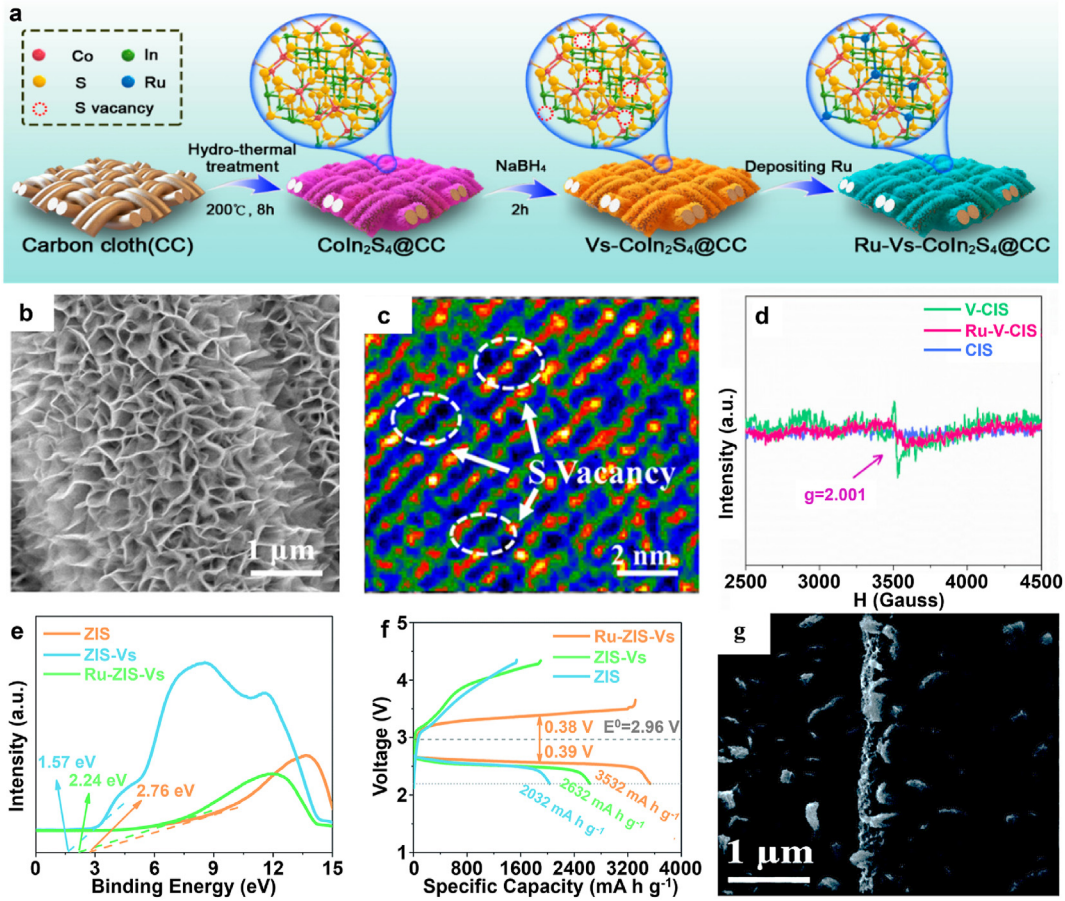

Fig. 6. (a) Schematic illustration for the synthesis of Ru-V-CIS. (b) SEM image of Ru-V-CIS. (c) False-color HRTEM image. (d) EPR spectra of Ru-V-CIS. Reprinted with permission of Ref. [49], copyright 2021 American Chemical Society. (e) XPS valence band spectra of ZIS, ZIS-Vs and Ru-ZIS-Vs. (f) Initial full discharge-charge curves of ZIS, ZIS-Vs and Ru-ZIS-Vs electrodes. (g) SEM image of Ru-ZIS-Vs after the first discharge. Reprinted with permission of Ref. [50], copyright 2020 The Royal Society of Chemistry.

and unsaturated coordination structure (Fig. 6d). The unsaturated coordination Ru-Co active center at the Ru/CIS interface can deliver asymmetrical electron donation to O_2 and Li_2O_2, accelerating the charge transfer and heighten the performance of Li-O_2 batteries.

In addition, Liang et al. prepared Ru/$ZnIn_2S_4$ (Ru-ZIS-Vs) modified surface sulfur-vacancies (Vs) Mott-Schottky heterojunctions as electrocatalysts for Li-O_2 batteries [50]. Sulfur vacancies combine with the doped Ru to construct a metal/semiconductor interface, improving its catalytic activity. Besides, the Ru-ZIS-Vs displays the smaller valence band (VB) value compared to ZIS, and the blue shift of VB derived from the S vacancies suggests that the charge transfer is promoted, exhibiting low discharge/charge overpotentials (0.39 V/0.38 V) and large discharge capacity of 3532 mAh·g^{-1} (Fig. 6e and f). The toroidal Li_2O_2 is formed on the Ru-ZIS-Vs and disappeared after the charge, displaying the high reversibility of the Ru-ZIS-Vs-based Li-O_2 batteries (Fig. 6g). Therefore, adjusting the interfacial electronic structure of AB_2S_4 is a strategy to elevate the performance of Li-O_2 batteries.

2.5. Ru single atoms

Single-atom catalysts (SACs) with metal atoms occupying single active sites upon solid supports have been applied in various catalytic domains due to their high reactivity and selectivity, unsaturated coordination structure and maximum atomic utilization [51,52]. The Ru SACs possessed the maximum atomic utilization rate are expected to absorb the discharge product Li_2O_2 and improve the reaction kinetics of ORR and OER. Therefore, it is crucial to design and explore Ru SACs to boost the electrochemical performance of Li-O_2 batteries and understand the reaction mechanism of SACs applied in their application.

Hu et al. synthesized zeolitic imidazolate frameworks (ZIF-8) and partially replaced Zn^{2+} nodes with Ru^{3+} as precursors, then they calcined the Ru-doped precursors at 900 °C to obtain Ru single atoms distributed in nitrogen (N)-doped porous carbon (Ru SAs-NC) (Fig. 7a) [53]. The Ru atoms are dispersed within the $Ru_{0.3}$ SAs-NC (Fig. 7b and c) and can coordinate with N atoms to form Ru-N_4 bonds compared to the Ru nanoparticles on N-doped carbon (Ru NPs-NC) (Fig. 7d and g). DFT

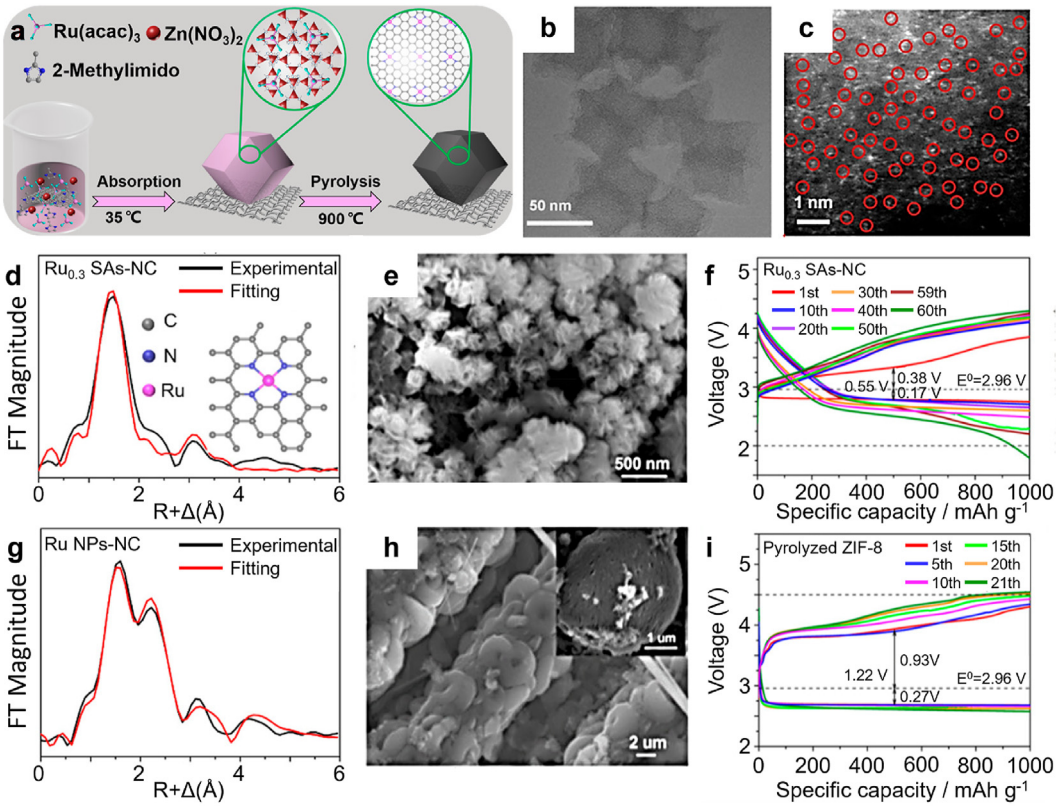

Fig. 7. (a) Scheme of the formation of Ru SAs-NC on the flexible CC. (b) TEM image of $Ru_{0.3}$ SAs-NC. (c) HAADF-STEM image of $Ru_{0.3}$ SAs-NC (Ru single atoms are marked with red circles). Corresponding EXAFS fitting curves at R space for (d) $Ru_{0.3}$ SAs-NC and (g) Ru NPs-NC. Inset e, schematic model (purple, blue, and gray balls stand for Ru, N, C, respectively). SEM images of (e) $Ru_{0.3}$ SAs-NC and (h) pyrolyzed ZIF-8 after discharge. Discharge-charge curves of (f) $Ru_{0.3}$ SAs-NC, and (i) pyrolyzed ZIF-8 electrodes with a fixed capacity of 1000 mAh·g^{-1} at a current density of 0.02 mA·cm^{-2} in the voltage window of 2.0—4.5 V. Reprinted with permission of Ref. [53], copyright 2020 American Chemical Society.

calculations reveal that the Ru-N_4 moiety, serving as the active center, significantly influences the electron density distribution, modulating the affinity with LiO_2. That is beneficial for the growth of the flower-like Li_2O_2 on the surface of the $Ru_{0.3}$ SAs-NC (Fig. 7e). The flower-like Li_2O_2 can be readily decomposed to accelerate the OER kinetics of the Li-O_2 batteries, resulting in the lower discharge/charge overpotential (0.38 V) and improved the cycle life (60 cycles) (Fig. 7f). Compared with $Ru_{0.3}$ SAs-NC, typical toroidal Li_2O_2 grown on the pyrolyzed ZIF-8 leads to the larger discharge/charge overpotential (1.22 V) and inferior cycling performance (21 cycles) in Li-O_2 batteries (Fig. 7h and i). These results indicate that the Ru-N_4 structure as active sites facilities the reversible formation and decomposition of Li_2O_2, thereby enhancing the ORR and OER kinetics of Li-O_2 batteries. However, isolated atoms are prone to aggregation due to their high surface energy [54]. Two-dimensional (2D) layered graphene materials have garnered extensive study owing to their high electrical conductivity and large surface area [55]. The structural defects caused by doping heteroatoms at the edges of graphene are considered to be one of the promising candidates for anchoring single atoms [56]. Xu's group employed an impregnation method to anchor Ru single atoms on N-doped reduced graphene oxide nanosheets (Ru-N/rGO) [57]. The N atoms provide efficient sites for anchoring single-atom Ru. The Li_2O_2 nanosheets are formed on the surface of Ru-N/rGO after discharging, and these nanosheets disappear after charging. The DFT simulations indicate that the combination of Ru single atoms and N heteroatoms defects creates efficient catalytic active sites for the formation and decomposition of Li_2O_2. This accelerates the reaction kinetics of ORR and OER in Li-O_2 battery.

2.6. Ru-based MOF and its derivatives

Metal-organic frameworks (MOFs) formed through the coordinated interaction between inorganic centers (metal ions or metal-containing clusters) and organic linkers have been widely applied in electrocatalytic field [58,59]. They possess open metal sites to capture O_2 as well as open channels for O_2 diffusion [60]. However, the intrinsic insulation of traditional MOFs restricts their electrocatalytic performance and leads to high charge overvoltages. Over the past decade, a novel class of conductive MOFs assembled with electron-donating ligands have been progressing rapidly. They are constructed via "through-space", "through-bond", and "extended conjugation" approaches, and the third approach guarantees best electric conductivity [61]. These conductive MOFs can accelerate the charge transfer between metal nodes and oxygen, and then regulate the adsorption of superoxide species [62]. This significantly enhances cathode kinetics in Li-O_2 batteries.

Recently, Li's group directly grew Ni-HTP nanowire arrays on carbon paper as electrodes by the coordination of Ni^{2+} with 2,3,6,7,10,11-hexaiminotriphenylene (HTP) in a hydrothermal reaction, and then partially replaced Ni sites with Ru via an ion-exchange method for NiRu-HTP [63]. The NiRu-HTP catalyst with the layered graphene-like honeycomb structure shows nanoarrays grown on the carbon paper and exhibits high crystalline features, as displayed in Fig. 8a–c. This conductive MOF ensures a unique reaction mechanism for Li-O_2 battery, as proposed in Fig. 8d and g. During discharging, Ru-N_4 on the NiRu-HTP strongly absorbs O_2 and accepts electrons for LiO_2 facilitated by its tunable d-band center. The strong absorption between LiO_2 and Ru-N_4 causes high local concentration around NiRu-HTP, fostering the production of film-like Li_2O_2 (Fig. 8e). This film-like Li_2O_2 is beneficial for electron transfer and ion diffusion on the cathode electrolyte interface, promoting its decomposition during charging. Conversely, LiO_2 tends to be dissolved in electrolytes and disproportionate for large toroidal Li_2O_2 due to the weak adsorption capability of LiO_2 on Ni-HTP. (Fig. 8h). The large toroidal Li_2O_2 can be oxidized by suffering from high charge overvoltages because the toroidal particles are remote from the catalytic active surface (Fig. 8i). Therefore, the NiRu-HTP-based Li-O_2 batteries demonstrate the superior rate capability compared to the Ni-HTP-based Li-O_2 batteries, indicating that the ORR and OER performances of Li-O_2 batteries are boosted (Fig. 8f).

MOF derivatives have been utilized as ORR electrocatalysts in fuel batteries and aqueous Zn-air batteries, which effectively promotes the formation and decomposition of products at solid-liquid interfaces [64,65]. Different from a solid-liquid interface, an insulative Li_2O_2 as a solid product is deposited on the cathode surface of the Li-O_2 batteries, leading to the formation of solid-solid interface between catalysts and Li_2O_2. Therefore, the design of electrocatalyst in the Li-O_2 batteries should not only focus on the ORR, but also consider the spatial dispersion of Li_2O_2 on catalyst surface. The preferable spatial dispersion is beneficial to increasing the interface contact between the catalyst and Li_2O_2, promoting the decomposition of Li_2O_2. Ru-based MOF derivatives possess unique three-dimensional (3D) structure and the strong adsorption for O_2^- intermediate. Li_2O_2 formed during discharge presents

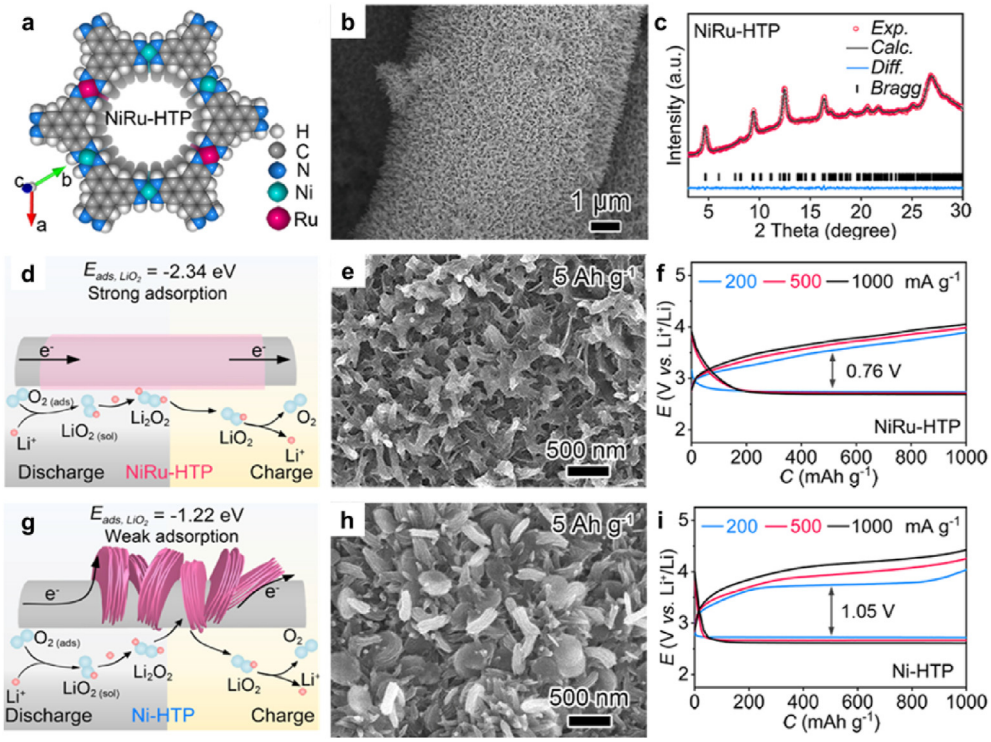

Fig. 8. (a) Simulated structure along c-axis, (b) SEM image, (c) Powder XRD and Pawley refinement patterns of NiRu-HTP. (d) The proposed reaction mechanism of NiRu-HTP. (e) SEM image of discharge NiRu-HTP cathode. (f) The rate performance of NiRu-HTP cathode. (g) The proposed reaction mechanism of Ni-HTP. (h) SEM image of discharge Ni-HTP cathode. (i) The rate performance of Ni-HTP cathode. Reprinted with permission of Ref. [63], copyright 2022 American Chemical Society.

good spatial dispersion on the Ru-based MOF derivatives. This helps to increase the contact area between the Li_2O_2 and Ru-based MOF derivatives, ultimately improving the reversibility of Li-O_2 batteries.

Yao et al. proposed a hollow dodecahedral carbon material with FeN_x moieties by pyrolysis of MOF, and further modified it by Ru nanoparticles (FeN_x-HDC@Ru) [66]. The internal network-like hollow structure of the material facilitates electron transport. Meanwhile, a relatively low impedance of Li_2O_2/catalyst contact interface is achieved by the synergistic effect of FeN_x moieties and Ru nanoparticles, accelerating the formation and decomposition of Li_2O_2 during discharging and charging. In order to further understand the mechanism of promoting interfacial contact through Ru-based MOF derivatives, Tong et al. synthesized Ru-modified nitrogen-doped porous carbon-encapsulated Co nanoparticles (Ru/Co@CoN_x-C) by precisely controlling the pyrolysis kinetics of a MOF precursor, which exhibits typical shrinking dodecahedron structure (Fig. 9a and b) [67]. The Ru/Co@CoN_x-C particles are enveloped by film-like Li_2O_2 (Fig. 9d), which facilitates full contact between Li_2O_2 and catalytic active sites, thereby enhancing the oxidation kinetics of Li_2O_2. The mechanism of Li_2O_2 formation and decomposition on the Ru/Co@CoN_x-C and Co@CoN_x-C is depicted to clarify the roles of Ru moiety and the Co@CoN_x-C moiety (Fig. 9e). During the discharge, O_2 initially forms LiO_2 intermediates which uniformly bind to the surface of the Ru/Co@CoN_x-C polyhedron via a one-electron reduction reaction. Subsequently, the LiO_2 intermediates are converted to a film-like Li_2O_2 by either the disproportionation reaction or the second one-electron reduction reaction due to the strong adsorption of LiO_2 (E_{ads} = −4.30 eV) on the Ru/Co@CoN_x-C polyhedron surface (Fig. 9c and d). During the charge, a reduced charge overpotential is attained owing to the substantial interfacial contact area between the Li_2O_2 and the catalytic active sites of Ru/Co@CoN_x-C catalyst, resulting in the complete decomposition of Li_2O_2. Compared with Ru/Co@CoN_x-C, the larger sawtooth-shaped Li_2O_2 particles are deposited on the Co@CoN_x-C surface due to the lower affinity between LiO_2 and the Co@CoNx-C particles (E_{ads} = −4.23 eV). The high polarization and poor stability are caused because such bulky Li_2O_2 is very difficult to be decomposed. As the result, the interfacial contact between Li_2O_2 and Ru modified TM-N-C is regulated. The Li-O_2 batteries based on the Ru/Co@CoN_x-C cathode exhibited a stable cycling performance of 205 cycles at a rate of 300 mA·g^{-1} (Fig. 9f).

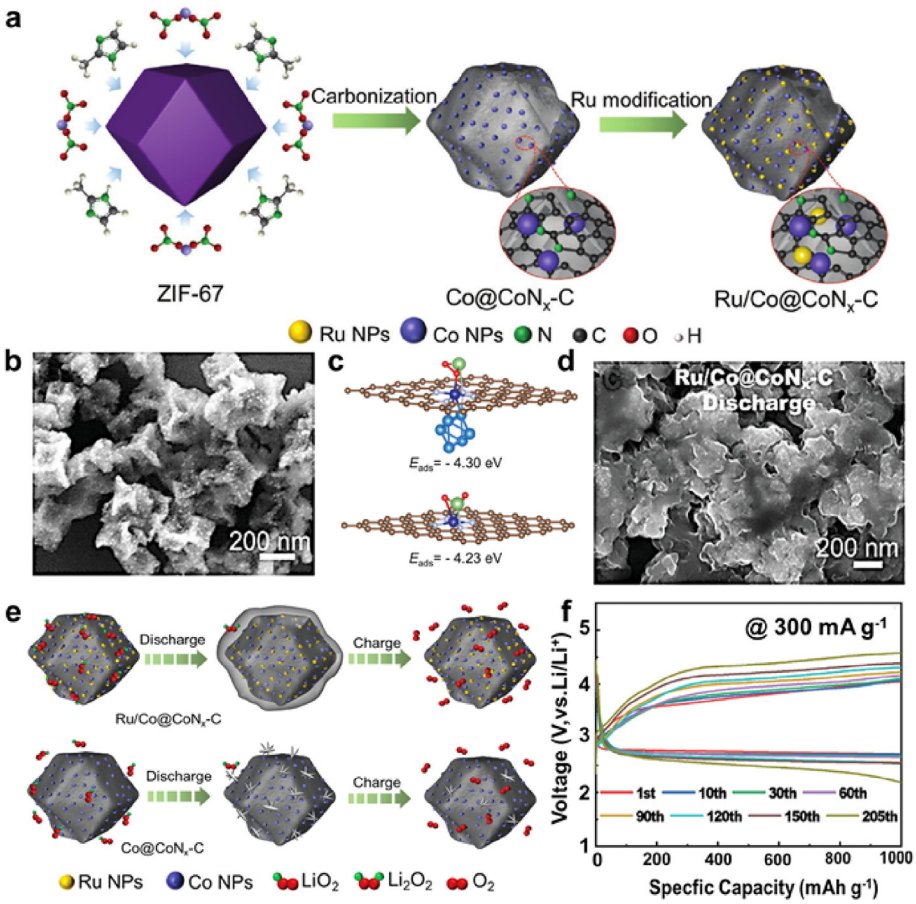

Fig. 9. (a) Scheme illustrating the preparations of Co@CoN_x-C and Ru/Co@CoN_x-C composites. (b) SEM images of Ru/Co@CoN_x-C. (c) The optimized configuration of LiO_2 adsorbed on the Co-N_4 site with or without the presence of Ru. (d) First discharged Ru/Co@CoN_x-C electrode. (e) Schematic illustrations to compare the formations and decompositions of discharge products on Ru/Co@CoN_x-C and Co@CoN_x-C electrodes. (f) Discharge-charge profiles of Ru/Co@CoN_x-C based electrode with different cycles at 300 mA·g^{-1}. Reprinted with permission of Ref. [67], copyright 2022 Wiley-VCH.

3. Conclusions and outlook

Aprotic Li-O_2 batteries have attracted significant attention due to their high theoretical energy density, but the sluggish cathode kinetics hinders their practical application. Ru-based compounds have been introduced as cathode catalysts due to their controllable morphology and electronic structure. These characteristics enable the adjustment of intermediate adsorption and modification of discharge product morphology. This review provides a comprehensive overview of the design and modulation of Ru-based compounds catalysts to enhance electrochemical performance in Li-O_2 batteries, such as: Ru metal or alloys, the incorporation Ru-based compounds into carbon materials, metal or metal oxides, metal sulfides, Ru single atoms and Ru-based MOF and its derivatives. It has been reported that these Ru-based compounds catalysts enhance ORR/OER activity, inhibit the formation of undesirable by-products, regulate the adsorption for LiO_2 by surface/interface engineering and establish favorable interfacial contact with Li_2O_2. The reversibility and cycling stability performance of Li-O_2 batteries are greatly improved due to these benefits of Ru-based compounds. However, Li-O_2 batteries still face numerous challenges, like the lithium metal anodes, electrolyte, cathode (i.e., solid catalyst), and additive (i.e., redox mediators) [68].

1) Most current literatures suggest that the active sites of catalyst can regulate the affinity of LiO_2 and facilitate charge transfer between the electrode and the discharge products. However, further research is necessary to fully understand the catalytic mechanism of the catalyst, and the processes of formation and decomposition of Li_2O_2. Technologies have been used to understand the catalytic mechanism of Ru-based electrocatalysts. For example, *in-situ* differential electrochemical mass spectrometry (DEMS) can monitor the O_2 consumption and release it in the discharge and charge processes. The affinity of the catalyst to LiO_2 can be revealed by electron paramagnetic resonance (EPR). Electrospray ionization mass spectrometry (ESI-MS) can identify the

intermediate in the catalysts-mediated reaction process. This deeper understanding is paramount for designing more efficient cathode catalysts.

2) The stability of Li-O_2 batteries heavily relies on the performance of lithium metal anodes. The growth of Li dendrites and side reactions triggered by O_2, H_2O and intermediates have hindered the reversibility of lithium metal anodes. It is very significant to develop an effective strategy to protect Li metal anodes in Li-O_2 batteries [69−71].

3) The electrolyte is one of the pivotal factors ensuring the operation of Li-O_2 batteries. The inevitable decomposition of organic electrolytes induced by reactive oxygen species has reduced the cycle stability of Li-O_2 batteries [72,73]. Therefore, the electrolyte in Li-O_2 batteries must possess the dual capability of stabilizing the lithium anode, and withstanding superoxide attack and decomposition facilitated by the presence of the catalyst.

Finally, comprehensive consideration of the cathode, lithium anode, and electrolyte is essential in the design of practical Li-O_2 batteries.

Conflict of interest

The authors decline no competing interest.

Acknowledgements

We are grateful for financial support from the National Natural Science Foundation of China (22325902 and 51671107) and Haihe Laboratory of Sustainable Chemical Transformations.

References

[1] Liu T, Vivek J P, Zhao E W, Lei J, Garcia-Araez N, Grey C P. Current challenges and routes forward for nonaqueous lithium-air batteries[J]. Chem. Rev., 2020, 120(14): 6558−6625.

[2] Du D F, Zhu Z, Chan K Y, Li F J, Chen J. Photoelectrochemistry of oxygen in rechargeable Li-O_2 batteries [J]. Chem. Soc. Rev., 2022, 51: 1846.

[3] Girishkumar G, McCloskey B, Luntz A C, Swanson S, Wilcke W. Lithium-air battery: promise and challenges[J]. J. Phys. Chem. Lett., 2010, 1(14): 2193−2203.

[4] Lu Y C, Gallant B M, Kwabi D G, Harding J R, Mitchell R R, Whittingham M S, Shao-Horn Y. Lithium-oxygen batteries: bridging mechanistic understanding and battery performance[J]. Energy Environ. Sci., 2013, 6(3): 750−768.

[5] Jiang Z L, Wen B, Huang Y H, Guo Y H, Wang Y Z, Li F J. New reaction pathway of superoxide disproportionation induced by a soluble catalyst in Li-O_2 batteries[J]. Angew. Chem. Int. Ed., 2024, 63(1): e202315314.

[6] Wandt J, Jakes P, Granwehr J, Gasteiger H A, Eichel R A. Singlet oxygen formation during the charging process of an aprotic lithium-oxygen battery[J]. Angew. Chem. Int. Ed., 2016, 55(24): 6892−6895.

[7] Jiang Z L, Xu G L, Yu Z, Zhou T H, Shi W K, Luo C S, Zhou H J, Chen L B, Sheng W J, Zhou M X, Cheng L, Assary R S, Sun S G, Sun H. High rate and long cycle life in Li-O_2 batteries with highly efficient catalytic cathode configured with Co_3O_4 nanoflower[J]. Nano Energy, 2019, 64: 103896.

[8] Wen B, Zhu Z, Li F J. Advances and challenges on cathode catalysts for lithium oxygen batteries[J]. J. Electrochem., 2023, 29(2): 7−19.

[9] Zahoor A, Ghouri Z K, Hasmi S, Raza F, Ishtiaque S, Nadeem S, Ullah I, Nahm K S. Electrocatalysts for lithium-air batteries: current status and challenges[J]. ACS Sustain. Chem. Eng., 2019, 7(17): 14288−14320.

[10] Zhao T, Yao Y, Yuan Y F, Wang M L, Wu F, Amine K, Lu J. A universal method to fabricating porous carbon for Li-O_2 battery[J]. Nano Energy, 2021, 82: 105782.

[11] Zhao B, Ye Z M, Kong X B, Han L, Xia Z Y, Chen K, Wang Q, Li M, Shang Y Y, Cao A Y. Orthogonal-channel, low-tortuosity carbon nanotube platforms for high-performance Li-O_2 batteries[J]. ACS Nano, 2023, 17(18): 18382−18391.

[12] Tu Y C, Deng D H, Bao X H. Nanocarbons and their hybrids as catalysts for non-aqueous lithium-oxygen batteries [J]. J. Energy Chem., 2016, 25(6): 957−966.

[13] Zhou Y, Yin K, Gu Q F, Tao L, Li Y J, Tan H, Zhou J H, Zhang W S, Li H B, Guo S J. Lewis-acidic PtIr multipods enable high-performance Li-O_2 batteries[J]. Angew. Chem. Int. Ed., 2021, 60(51): 26592−26598.

[14] Barile C J, Gewirth A A. Investigating the Li-O_2 battery in an ether-based electrolyte using differential electrochemical mass spectrometry[J]. J. Electrochem. Soc., 2013, 160(4): A549.

[15] Jung H G, Jeong Y S, Park J B, Sun Y K, Scrosati B, Lee Y J. Ruthenium-based electrocatalysts supported on reduced graphene oxide for lithium-air batteries[J]. ACS Nano, 2013, 7(4): 3532−3539.

[16] Yang Y, Liu W, Wu N A, Wang X C, Zhang T, Chen L F, Zeng R, Wang Y M, Lu J T, Fu L, Li X, Zhuang L. Tuning the morphology of Li_2O_2 by noble and 3d metals: a planar model electrode study for Li-O_2 battery[J]. ACS Appl. Mater. Interfaces, 2017, 9(23): 19800−19806.

[17] Bae Y, Park H, Ko Y, Kim H, Park S K, Kang K. Bifunctional oxygen electrocatalysts for lithium-oxygen batteries[J]. Batteries Supercaps, 2019, 2(4): 311−325.

[18] Zhang M, Zou L, Yang C Z, Chen Y, Shen Z R, Chi B. An all-nanosheet OER/ORR bifunctional electrocatalyst for both aprotic and aqueous Li-O_2 batteries[J]. Nanoscale, 2019, 11(6): 2855−2862.

[19] Vankova S, Francia C, Amici J, Zeng J, Bodoardo S, Penazzi N, Collins G, Geaney H, O'Dwyer C. Influence of binders and solvents on stability of Ru/RuO_x nanoparticles on ITO nanocrystals as Li-O_2 battery cathodes[J]. ChemSusChem, 2017, 10(3): 575−586.

[20] Jung C Y, Zhao T S, Zeng L, Tan P. Vertically aligned carbon nanotube-ruthenium dioxide core-shell cathode for non-aqueous lithium-oxygen batteries[J]. J. Power Sources, 2016, 331: 82−90.

[21] Kwak K H, Kim D W, Kang Y, Suk J. Hierarchical Ru-and RuO_2-foams as high performance electrocatalysts for rechargeable lithium-oxygen batteries[J]. J. Mater. Chem. A, 2016, 4(42): 16356−16367.

[22] Yang J B, Mi H W, Luo S, Li Y L, Zhang P X, Deng L B, Sun L N, Ren X Z. Atomic layer deposition of TiO_2 on nitrogen-doped carbon nanofibers supported Ru nanoparticles for flexible Li-O_2 battery: a combined DFT and experimental study[J]. J. Power Sources, 2017, 368: 88−96.

[23] Li F J, Chen Y, Tang D M, Jian Z L, Liu C, Golberg D, Yamada A, Zhou H S. Performance-improved Li-O_2 battery with Ru nanoparticles supported on binder-free multiwalled carbon nanotube paper as cathode[J]. Energy Environ. Sci., 2014, 7(5): 1648−1652.

[24] Wu D F, Guo Z Y, Yin X B, Pang Q Q, Tu B B, Zhang L J, Wang Y G, Li Q W. Metal-organic frameworks as cathode materials for Li-O_2 batteries[J]. Adv. Mater., 2014, 26(20): 3258−3262.

[25] Su D W, Dou S X, Wang G X. Hierarchical Ru nanospheres as highly effective cathode catalysts for Li-O_2 batteries[J]. J. Mater. Chem. A, 2015, 3(36): 18384−18388.

[26] Ma S C, Wu Y, Wang J W, Zhang Y L, Zhang Y T, Yan X X, Wei Y, Liu P, Wang J P, Jiang K L, Fan S S, Xu Y, Peng Z Q. Reversibility of noble metal-catalyzed aprotic Li-O_2 batteries[J]. Nano Lett., 2015, 15(12): 8084−8090.

[27] Kim J G, Kim Y, Noh Y, Lee S, Kim Y, Kim W B. Bifunctional hybrid catalysts with perovskite $LaCo_{0.8}Fe_{0.2}O_3$ nanowires and reduced graphene oxide sheets for an efficient Li-O_2 battery cathode[J]. ACS Appl. Mater. Interfaces, 2018, 10(6): 5429−5439.

[28] Lin Y, Moitoso B, Martinez-Martinez C, Walsh E D, Lacey S D, Kim J W, Dai L, Hu L, Connell J W. Ultrahigh-capacity lithium-oxygen batteries enabled by dry-pressed holey graphene air cathodes[J]. Nano Lett., 2017, 17(5): 3252−3260.

[29] Zhong X, Papandrea B, Xu Y X, Lin Z Y, Zhang H, Liu Y, Huang Y, Duan X F. Three-dimensional graphene membrane cathode for high energy density rechargeable lithium-air batteries in ambient conditions[J]. Nano Res., 2017, 10: 472−482.

[30] Sun B, Munroe P, Wang G X. Ruthenium nanocrystals as cathode catalysts for lithium-oxygen batteries with a superior performance[J]. Sci. Rep., 2013, 3(1): 2247.

[31] Sun B, Chen S Q, Liu H, Wang G X. Mesoporous carbon nanocube architecture for high-performance lithium-oxygen batteries[J]. Adv. Funct. Mater., 2015, 25(28): 4436−4444.

[32] Song H Y, Xu S M, Li Y J, Dai J Q, Gong A, Zhu M W, Zhu C L, Chen C J, Chen Y A, Yao Y G, Liu B Y, Song J W, Pastel G, Hu L B. Hierarchically porous, ultrathick, "breathable" wood-derived cathode for lithium-oxygen batteries[J]. Adv. Energy Mater., 2018, 8(4): 1701203.

[33] Liu M R, Sun K L, Zhang Q H, Tang T, Huang L L, Li X H, Zeng X, Y Hu J S, Liao S J. Rationally designed three-dimensional N-doped graphene architecture mounted with Ru nanoclusters as a high-performance air cathode for lithium-oxygen batteries[J]. ACS Sustain. Chem. Eng., 8(15): 6109−6117.

[34] Dai W R, Liu Y, Wang M, Lin M, Lian X, Luo Y N, Yang J L, Chen W. Monodispersed ruthenium nanoparticles on nitrogen-doped reduced graphene oxide for an efficient lithium-oxygen battery[J]. ACS Appl. Mater. Interfaces, 2021, 13(17): 19915−19926.

[35] Sun Z, Yang C S, Jiang F L, Zhang T. Chimerism of carbon by ruthenium induces gradient catalysis[J]. Adv. Funct. Mater., 2021, 31(34): 2104011.

[36] Cao D Q, Zhang S S, Yu F J, Wu Y P, Chen Y H. Carbon-free cathode materials for Li-O_2 batteries[J]. Batteries Supercaps, 2019, 2(5): 428−439.

[37] Li F J, Tang D M, Chen Y, Golberg D, Kitaura H, Zhang T, Yamada A, Zhou H S. Ru/ITO: a carbon-free cathode for nonaqueous Li-O_2 battery[J]. Nano lett., 2013, 13(10): 4702−4707.

[38] Li F J, Tang D M, Jian Z L, Liu D Q, Golberg D, Yamada A, Zhou H S. Li-O_2 battery based on highly efficient Sb-doped tin oxide supported Ru nanoparticles[J]. Adv. Mater., 2014, 26(27): 4659−4664.

[39] Xu Y F, Chen Y, Xu G L, Zhang R X, Chen Z, Li J T, Huang L, Amine K, Sun S G. RuO_2 nanoparticles supported on MnO_2 nanorods as high efficient bifunctional electrocatalyst of lithium-oxygen battery[J]. Nano Energy, 2016, 28: 63−70.

[40] Wu X B, Zhang Y F, Chen S Y, Zhan X Y, Zhang H, Zhang L, Su L W, Shen C Q, Chen H, Wu H, Wang L B. Low-carbon CeO_x/Ru@RuO_2 nanosheets as bifunctional catalysts for lithium-oxygen batteries[J]. J. Alloys Compd., 2022, 924: 166354.

[41] Zhang S Q, Wang Y, Li D, Kang Z Y, Dong F L, Xie H M, Liu J. Ru-impregnated needle-like $NiCo_2O_4$ embedded in carbon textiles as O_2 electrode for a flexible Li-O_2 battery[J]. J. Alloys Compd., 2020, 825: 154054.

[42] Zou L, Jiang Y X, Cheng J F, Chen Y, Chi B, Pu J, Jian L. Bifunctional catalyst of well-dispersed RuO_2 on $NiCo_2O_4$ nanosheets as enhanced cathode for lithium-oxygen batteries[J]. Electrochim. Acta, 2018, 262: 97−106.

[43] Yoon K R, Kim D S, Ryu W H, Ryu W H, Song S H, Youn D Y, Jung J W, Jeon S, Park Y J, Kim I D. Tailored combination of low dimensional catalysts for efficient oxygen reduction and evolution in Li-O_2 batteries[J]. ChemSusChem, 2016, 9(16): 2080−2088.

[44] Yoon K R, Lee G Y, Jung J W, Kim N H, Kim S O, Kim I D. One-dimensional RuO_2/Mn_2O_3 hollow architectures as efficient bifunctional catalysts for lithium-oxygen batteries [J]. Nano Lett., 2016, 16(3): 2076−2083.

[45] Lian Z, Lu Y C, Zhao S Z, Li Z J, Liu Q C. Engineering the electronic interaction between atomically dispersed Fe and RuO_2 attaining high catalytic activity and durability catalyst for Li-O_2 battery[J]. Adv. Sci., 2023, 10(9): 2205975.

[46] Kulkarni P, Nataraj S K, Balakrishna R G, Nagarajua D H, Reddy M V. Nanostructured binary and ternary metal sulfides: synthesis methods and their application in energy conversion and storage devices[J]. J. Mater. Chem. A, 2017, 5(42): 22040−22094.

[47] Chandrasekaran S, Yao L, Deng L, Bowen C, Zhang Y, Chen S, Lin Z, Peng F, Zhang P. Recent advances in metal sulfides: from controlled fabrication to electrocatalytic, photocatalytic and photoelectrochemical water splitting and beyond[J]. Chem. Soc. Rev., 2019, 48(15): 4178−4280.

[48] Fu G T, Wang J, Chen Y F, Liu Y, Tang Y W, Goodenough J B, Lee J M. Exploring indium-based ternary thiospinel as conceivable high-potential air-cathode for rechargeable Zn-Air batteries[J]. Adv. Energy Mater., 2018, 8(31): 1802263.

[49] Zheng R X, Shu C Z, Liu C H, Yan Y, He M, Li M L, Hu A J, Long J P. Tuning the unsaturated coordination center of electrocatalysts toward high-performance lithium-oxygen batteries[J]. ACS Sustain. Chem. Eng., 2021, 9(22): 7499−7507.

[50] Liang R X, Shu C Z, Hu A J, Xu C X, Zheng R X, Li M L, Guo Y W, He M, Yan Y, Long J P. Tuning the electronic band structure of mott-Schottky heterojunctions modified with surface sulfur vacancy achieves an oxygen electrode with high catalytic activity for lithium-oxygen batteries[J]. J. Mater. Chem. A, 2020, 8(22): 11337−11345.

[51] Wang Y, Mao J, Meng X G, Yu L, Deng D H, Bao X H. Catalysis with two-dimensional materials confining single atoms: concept, design, and applications[J]. Chem. Rev., 2018, 119(3): 1806−1854.

[52] Cao L L, Luo Q Q, Chen J J, Wang L, Lin Y, Wang H J, Liu X K, Shen X Y, Zhang W, Liu W, Qi Z M, Jiang Z, Yang J L, Yao T. Dynamic oxygen adsorption on single-atomic ruthenium catalyst with high performance for acidic oxygen evolution reaction[J]. Nat. Commun., 2019, 10(1): 4849.

[53] Hu X L, Luo G, Zhao Q N, Wu D, Yang T X, Wen J, Wang R H, Xu C H, Hu N. Ru single atoms on N-doped carbon by spatial confinement and ionic substitution strategies for high-performance Li-O_2 batteries[J]. J. Am. Chem. Soc., 2020, 142(39): 16776−16786.

[54] Dhiman M, Polshettiwar V. Supported single atom and pseudo-single atom of metals as sustainable heterogeneous nanocatalysts[J]. ChemCatChem, 2018, 10(5): 881−906.

[55] Alaf M, Tocoglu U, Kartal M, Akbulut H. Graphene supported heterogeneous catalysts for Li-O_2 batteries[J]. Appl. Surf. Sci., 2016, 380: 185−192.
[56] Ren S, Yu Q, Yu X H, Rong P, Jiang L Y, Jiang J C. Graphene-supported metal single-atom catalysts: a concise review[J]. Sci. China Mater., 2020, 63(6): 903−920.
[57] Liu W Y, Su Q M, Yu L T, Du G H, Li C X, Zhang M, Ding S K, Xu B S. Understanding reaction mechanism of oxygen evolution reaction using Ru single atoms as catalyst for Li-O_2 battery[J]. J. Alloys Compd., 2021, 886: 161189.
[58] He J, Zha M Q, Cui J S, Zeller M, Hunter A D, Yiu S M, Lee S T, Xu Z. T Convenient detection of Pd(II) by a metal-organic framework with sulfur and olefin functions[J]. J. Am. Chem. Soc., 2013, 135(21): 7807−7810.
[59] Xiao L Y, Wang Z L, Guan J Q. 2D MOFs and their derivatives for electrocatalytic applications: recent advances and new challenges[J]. Coord. Chem. Rev., 2022, 472: 214777.
[60] Meng Z H, Chen N, Cai S C, Wang R, Wu J W, Tang H L. Recent advances of hierarchically porous bifunctional oxygen electrocatalysts derived from metal-organic frameworks for Zn-Air batteries[J]. Mater. Chem. Front., 2021, 5(6): 2649−2667.
[61] Jiang Z L, Wen B, Huang Y H, Li H X, Li F J. Metal-organic framework-based lithium-oxygen batteries[J]. Chem. Eur. J., 2022, 28(64): e202202130.
[62] Lv Q L, Zhu Z, Ni Y X, Geng J R, Li F J. Spin-state manipulation of two-dimensional metal-organic framework with enhanced metal-oxygen covalency for lithium-oxygen batteries[J]. Angew. Chem. Int. Ed., 2022, 61(8): e202114293.
[63] Lv Q L, Zhu Z, Ni Y X, Wen B, Jiang Z L, Fang H Y, Li F J. Atomic ruthenium-riveted metal-organic framework with tunable d-band modulates oxygen redox for lithium-oxygen batteries[J]. J. Am. Chem. Soc., 2022, 144(50): 23239−23246.
[64] Zhang M D, Dai Q B, Zheng H G, Chen M D, Dai L M. Novel MOF-derived Co@N-C bifunctional catalysts for highly efficient Zn-air batteries and water splitting[J]. Adv. Mater., 2018, 30(10): 1705431.
[65] Li Z Q, Yang J Y, Ge X L, Deng Y P, Jiang G P, Li H B, Sun G R, Liu W W, Zheng Y, Dou H Z, Jiao H L, Zhu J B, Li N, Hu Y F, Feng M, Chen Z W. Self-assembly of colloidal MOFs derived yolk-shelled microcages as flexible air cathode for rechargeable Zn-air batteries[J]. Nano Energy, 2021, 89: 106314.
[66] Yao L X, Lin J, Li S, Wu Y H, Ding H R, Zheng H F, Xu W J, Xie T, Yue G H, Peng D L. Metal-organic frameworks-derived hollow dodecahedral carbon combined with FeN_x moieties and ruthenium nanoparticles as cathode electrocatalyst for lithium-oxygen batteries[J]. J. Colloid Interface Sci., 2021, 596: 1−11.
[67] Tong Z, Lv C, Zhou Y, Zhang P F, Xiang C C, Li Z G, Wang Z, Liu Z K, Li J T, Sun S G. Highly dispersed Ru-Co nanoparticles interfaced with nitrogen-doped carbon polyhedron for high efficiency reversible Li-O_2 battery[J]. Small, 2022, 18(48): 2204836.
[68] Zhao S, Wang C C, Du D F, Li L, Chou S L, Li F J, Chen J. Bifunctional effects of cation additive on Na-O_2 batteries[J]. Angew. Chem. Int. Ed., 2021, 133(6): 3242−3248.
[69] Yu Y, Yin Y B, Ma J L, Chang Z W, Sun T, Zhu Y H, Yang X Y, Liu T, Zhang X B. Designing a self-healing protective film on a lithium metal anode for long-cycle-life lithium-oxygen batteries[J]. Energy Storage Mater., 2019, 18: 382−388.
[70] Huang Y H, Geng J R, Jiang Z L, Ren M, Wen B, Chen J, Li F J. Solvation structure with enhanced anionic coordination for stable anodes in lithium-oxygen batteries[J]. Angew. Chem. Int. Ed., 2023, 62(30): e202306236.
[71] Huang Y H, Wen B, Jiang Z L, Li F J. Solvation chemistry of electrolytes for stable anodes of lithium metal batteries[J]. Nano Res., 2023, 16(6): 8072−8081.
[72] Luntz A C, McCloskey B D. Li-air batteries: importance of singlet oxygen[J]. Nat. Energy, 2017, 2(5): 1−2.
[73] Jiang Z L, Huang Y H, Zhu Z, Gao S N, Lv Q L, Li F J. Quenching singlet oxygen via intersystem crossing for a stable Li-O_2 battery[J]. Proc. Natl. Acad. Sci. USA, 2022, 119(34): e2202835119.

锂氧电池中钌基电催化剂的研究进展

王昱喆[a]，蒋卓良[a]，温　波[a]，黄耀辉[a]，李福军[a,b,*]
[a]南开大学化学学院，先进能源材料化学教育部重点实验室，天津 300071
[b]天津物质绿色创造与制造海河实验室，天津 300192

摘要

可充电锂氧（Li-O_2）电池因其高能量密度而受到广泛关注。然而，缓慢的阴极动力学导致较高过电压和较差的循环性能。为了克服这一问题，不同种类的阴极催化剂已经开始被探索。其中，钌基电催化剂已被证明是促进析氧反应（OER）的极具前景的阴极催化剂。由于钌基催化剂与超氧根阴离子（O_2^-）中间体之间存在强相互作用，因此可以通过调节 Li_2O_2 的形态来促进过氧化锂（Li_2O_2）的分解。本文介绍了钌基电催化剂的设计策略，以提高其在锂氧电池中的 OER 催化动力学。不同结构的钌基催化剂已经被总结，包括金属颗粒（钌金属和合金）、单原子催化剂和不同底物（碳材料、金属氧化物/硫化物）负载钌的化合物，以调节钌基电催化剂的电子结构和基体结构。这些钌基电催化剂调节了对 LiO_2 的吸附，提高了 OER 活性，抑制了副产物的形成，从而提升了 Li-O_2 电池的可逆性和循环稳定性。然而，Li-O_2 电池仍然面临着许多挑战。其中之一是锂金属阳极的问题，锂的不稳定性和安全性一直是 Li-O_2 电池研究的一个关键问题。此外，电解质的选择和阴极材料的优化也是当前研究的重点之一。为了提高 Li-O_2 电池的性能，还需要对添加剂（即氧化还原介质）进行更深入的研究，以提高电池的循环寿命和能量密度。这些挑战的克服将需要跨学科的合作和持续的研究努力，以推动 Li-O_2 电池的进一步发展。

关键字：锂-氧电池；钌基电催化剂；反应机理；反应速率；过电压